Journal of Quaternary Science

Late glacial and Holocene landscape change and rapid climate and coastal impacts in the Canal Beagle, southernmost Patagonia.

Journal:	*Journal of Quaternary Science*
Manuscript ID	JQS-19-0064.R1
Wiley - Manuscript type:	Research Article
Date Submitted by the Author:	n/a
Complete List of Authors:	McCulloch, Robert; Centro de Investigación en Ecosistemas de la Patagonia (CIEP), Laboratorio Eco-climatico; The University of Edinburgh, School of GeoSciences Mansilla, Claudia; GAIA Universidad de Magallanes Morello, Flavia; Universidad de Magallanes, Centro de Estudios del Hombre Austral (CEHA), Instituto de la Patagonia De Pol-Holz, Ricardo; GAIA Universidad de Magallanes San Román, Manuel; Universidad de Magallanes, Centro de Estudios del Hombre Austral (CEHA), Instituto de la Patagonia Tisdall, Eileen; University of Stirling School of Natural Sciences, Biological & Environmental Sciences Torres, Jimena; Universidad de Magallanes, Centro de Estudios del Hombre Austral (CEHA), Instituto de la Patagonia
Keywords:	Pollen analysis, Tephrochronology, Sea-level change, Pollen preservation, Southern westerly winds

Late glacial and Holocene landscape change and rapid climate and coastal impacts in the Canal Beagle, southernmost Patagonia.

McCulloch, R.D[1,3]., Mansilla, C.A[2]., Morello, F[4]., De Pol-Holz, R[2]., San Román, M[4]., Tisdall, E[5]., Torres, J[4].

[1]Centro de Investigación de Ecosistemas de la Patagonia (CIEP), Coyhaique, Chile.

[2]Centro de Investigación Gaia Antártica (CIGA), Universidad de Magallanes, Punta Arenas, Chile.

[3]School of GeoSciences, University of Edinburgh, Edinburgh, Scotland, UK.

[4]Centro de Estudios del Hombre Austral (CEHA), Instituto de la Patagonia, Universidad de Magallanes, Punta Arenas, Chile.

[5]Biological & Environmental Sciences, University of Stirling, Stirling, Scotland, UK.

Abstract

Palaeoenvironmental data for the Late glacial and Holocene is provided from Caleta Eugenia, in the eastern sector of Canal Beagle, southernmost Patagonia. The record commences at c. 16,200 cal a BP following glacier retreat in response to climatic warming. However, cooler conditions persisted during the Late glacial period. The onset of more temperate conditions after c. 12,390 cal a BP is indicated by the arrival of southern beech forest and later establishment at c. 10,640 cal a BP, but the woodland growth was restricted by lower levels of effective moisture. The climate signal is then truncated by a rapid marine incursion at c. 8640 cal a BP which lasted until a more gradual emergence of the coast at c. 6600 cal a BP. During this period the pollen record appears to be dominated by the southern beech woodland. A punctuated hydroseral succession follows the isolation of the site from the sea leading to the re-establishment of a peat bog. Between c. 5770 cal a BP and the present there were several periods of short rapid climatic change leading to drier conditions, probably as a result of late Holocene periods of climatic warming.

Keywords: Pollen analysis, Tephrochronology, Sea-level change, Pollen preservation, Southern westerly winds.

1. Introduction

Climate of the south-eastern part of the Fuegian archipelago, southernmost Patagonia, is strongly influenced by the westerly atmospheric circulation, the southern westerly winds (SWWs). The intensity and location of the westerlies reflect the extent of Antarctic sea ice, the movements in the circumpolar oceanic Antarctic Convergence and the strength of sub-tropical anticyclonic cells over the Atlantic and Pacific Oceans (Moy et al., 2008). The steep climatic gradients and Andean topography of the Fuegian archipelago results in a complex mosaic of environments which range from maritime to alpine to continental conditions within tens of kilometres. Topography (highest point 2405 m a.s.l.) and climate combine to support extant ice fields on the Cordillera Darwin. The present vegetation of the region closely reflects the steep precipitation gradient from the hyper humid Magellanic moorland and evergreen forests in the west (mean annual precipitation ~3000-2000 mm a^{-1}) to the deciduous forests and steppe vegetation (mean annual precipitation ~500-300 mm a^{-1}) in the east (Fig. 1). The core of the present SWWs migrates seasonally but also probably migrated ~5° of latitude northwards during the Last Glacial Maximum (Hulton et al., 2002). Shifts in the latitudinal position of the SWWs during the Late glacial and Holocene would have driven shorter term regional changes in precipitation, generating complex vegetation and landscape responses. A chronologically well constrained palaeoenvironmental record of these landscape and vegetation dynamics can provide regional evidence for shifts in the position of the SWWs.

The Canal Beagle (54°54'S) is a west-east trending trough at the boundary between the South America and Scotia tectonic plates (Bujaleski 2011) (Fig. 1). The canal lies to the east of the Cordillera Darwin and has been repeatedly scoured by glacier advances draining the eastern ice divide of the cordillera during successive glacial cycles. During the Last Glacial Maximum (LGM) the Canal Beagle glacier likely advanced as far as Pta. Moat-Isla Picton (Rabassa et al., 2000) (Fig. 1). The timing of ice retreat of the Cordillera Darwin glaciers after the LGM is uncertain but there is evidence to suggest widespread retreat after c. 17,500 cal a BP (Rabassa et al., 2000; McCulloch et al., 2005; Hall et al., 2018) in response to regional warming reflected in the Antarctic ice cores (Jouzel et al., 2007). The isostatic legacy of the last glaciation is also evidenced by raised palaeoshorelines associated with ice dammed proglacial lakes and a raised Holocene marine shoreline (Borromei and Quattrocchio, 2007).

However, our ability to describe how such a heterogenous landscape responded to climate change, and in particular shifts in the SWWs, is limited by the geographic and temporal paucity of palaeoenvironmental records from the region. There are a number of Holocene palaeoecological records from the north of the Canal Beagle (Valle Andorra: Borromei, 1995; Punta (Pta.) Moat: Borromei et al., 2014) and a few that span the Late glacial - Holocene (Puerto (Pto.) Harberton: Markgraf and Huber, 2010; Ushuaia I, II and III: Heusser, 1998; Cañadón del Toro: Borromei et al., 2016; Terra Australis: Mussoto et al., 2017). Together these sites suggest a landscape that was treeless during the Late glacial and was generally colonised by *Nothofagus* (southern beech) woodland between c.10,500 and 10,300 cal a BP (see Mansilla et al., 2016 for a more comprehensive review). There is only one palaeoecological record from the south of the Canal Beagle (Caleta (Cta.) Robalo (aka Pto. Williams: Heusser, 1989) and one to the east on Isla de los Estados (Cta. Lacroix: Ponce and Fernandez, 2014). These records suggest that the position of the SWWs has shifted latitudinally during the Late glacial and Holcoene but there remains a lack of spatial definition of poleward shifts as well as poor temporal resolution. Here we present palaeoenvironmental evidence from a mire within an isolation basin located at the eastern end of the north shore of Isla Navarino (Canal Beagle), part of the Fuegian archipelago. Such sites are relatively rare, and the record will provide a climate sensitive, multi proxy record of environmental change and provide valuable insights into the evolution of the coastal margin in a post-glaciated area.

Several studies in the Canal Beagle have focused on Holocene marine transgression sites on the north side of the canal (Lapataia 1 and 2: Heusser, 1998; Borromei and Quattrocchio, 2007; Albufera Lanushuaia: Candela et al., 2011 and Rio Varela: Grill et al., 2002). The timing of the marine incursion is broadly c. 8800 to 6800 cal a BP. However, extent and duration of the mid-Holocene marine incursion and the potential disruptive effects of neotectonics movements remains uncertain (Borromei and Quattrocchio, 2007). A clearer definition of the mid-Holocene marine incursion is required as it is central to any interpretation of human colonisation and occupation of the region.

The human occupation of Tierra del Fuego dates from the Late glacial-Holocene transition and the earliest archaeological record is from Cueva Tres Arroyos 1, northern Tierra del Fuego, which indicates that humans had arrived by c. 12,000 cal a BP (Massone, 2004). Human activity was strongly related to terrestrial resources, mainly guanaco (*Lama guanicoe*) and the minor use of now extinct taxa (Martin, 2006). Along the southern coast of Tierra del Fuego, along the Canal Beagle, the earliest evidence for human occupation ranges between c. 8700 and 7300 cal a BP (lower layers of archaeological sites Túnel 1, Imiwaia and Binushmuka I (Bahía Cambaceres): Orquera and Piana 2009; Zangrando et al., 2019) (Fig. 1). Archaeological evidence from Isla Navarino suggests the coastal margins were colonized by early marine hunter-gatherer groups at c. 7000 cal a BP and this nomadic lifestyle persisted till the beginning of the twentieth century (Legoupil et al., 1993; Ocampo and Rivas, 2000; San Roman et al., 2017). Thus, understanding the environment-human dynamics along the coastal margins are key to understanding the nomadic peopling of the sub Antarctic region during the Holocene (McCulloch and Morello, 2009; Rozzi, 2012). The narrow strip of land that forms the coastal zone, including the near-shore highly productive ecosystems of kelp forests and diverse hotspots for marine resources (Cárdenas and Montiel, 2016), was an important geographical space for accessing marine and terrestrial resources (e.g. materials for diet, fuel, tools and shelter). The littoral setting is directly related to all past socio-cultural activity of the Canal Beagle inhabitants (San Roman, 2018). Thus, the palaeoenvironmental record from Cta. Eugenia may help us better understand the interactions between humans and their changing landscape ecosystems at the land-marine interface along the Canal Beagle channel during the Holocene

2. Material and methods

2.1. Study area

The site is a mire within a small depression near Cta. Eugenia (54°55'44.7"S, 67°20'44.5"W, altitude 3.7 m a.s.l.; Fig. 1). The surrounding landforms comprise glacial drift and were probably formed during the Last Glacial Maximum, when the glaciers expanded from the Cordillera Darwin and flowed eastwards along the Canal Beagle (Rabassa et al., 2000). The mire site is located between the open coastal landscape, including a series of storm beach ridges (the highest ridge reaches ~4.0 m a.s.l.), and dense forest (Fig. 2). There is an ephemeral linear pool of water that lies inland of the storm beach ridges and bounds the raised mire. The present vegetation suggests reduced mire surface wetness with *Empetrum rubrum* and *Chiliotrichium diffusum* scrub and *Nothofagus betuloides* and *Nothofagus antarctica* colonising the mire surface. Smaller wetter areas are dominated by hummocky *Sphagnum magellanicum*. The surrounding landscape is covered by *Festuca - Chiliotrichium* grass-scrub along the coastal margin and inland there is dense primary and secondary southern beech deciduous forest (*Nothofagus pumilio* and *Nothofagus antarctica*). The climate of Isla Navarino lies at the boundary between temperate humid with cool summers (Cfc) and Polar tundra (ET). Annual precipitation is ~500 mm a^{-1} with more falling in the austral summer months, and there is a seasonal difference in temperature, with a mean temperature in January (austral summer) of ~9.3°C and in July (austral winter) 1.8°C (Tuhkanen et al., 1989-1990).

2.3. Sediment coring and laboratory methods

A 900 cm core was retrieved from the mire using a 50 cm long Russian corer with a 5.5 cm diameter (Jowsey, 1966). Each core section was photographed and described in the field following Troels Smith (1955) with simplified lithology shown in figures for ease of reproduction. Core sections were then transferred to plastic guttering, sealed in polythene lay-flat tubing and stored at a constant 4°C at the University of Stirling.

The organic content of the core was estimated by loss-on-ignition with 2 cm contiguous sub-samples combusted for 4 hours at 550°C (LOI_{550}). Sub-samples of 1 cm^3 were taken from the core at a resolution of between 8 cm and 4 cm and prepared for pollen analysis using a standard methodology (Moore et al., 1991). Pollen, spores and algae were identified using an Olympus BX43 light microscope, at 400x magnification and a minimum of 300 total land pollen (TLP) were counted per sub-sample, the total excluding Cyperaceae, aquatics and spores. Known concentrations of *Lycopodium clavatum* spores were added to the samples to facilitate the estimation of the concentration of pollen, spores and algae (No. grains cm^{-3}) (Stockmarr, 1971). The concentration values and sediment accumulation rates (cm a^{-1}) were used to calculate the total pollen accumulation rate (pollen influx, No. grains cm^{-2} a^{-1}) and total charcoal accumulation rate (charcoal influx, No. particles cm^{-2} a^{-1}). The charcoal particles were counted and measured alongside the pollen and were classified into two categories by size ≤100 µm (microscopic) and 100-180 µm (macroscopic) (Whitlock and Larsen, 2001).

Pollen and spores were identified with the aid of a pollen reference collection (held by RMcC) supported by photographs of pollen and spores (Heusser, 1971; Wingenroth and Heusser, 1984; Moore et al., 1991). The palynological data was plotted using Tilia version 2.6.1 (Grimm, 2011). Local pollen assemblage zones (LPAZs) were determined using the stratigraphically constrained incremental sum-of-squares cluster analysis (CONISS, Grimm, 1987).

Additional insights into the changing environmental conditions at the site were obtained through the hierarchical categorization of the state of preservation of each land pollen grain: normal, broken, crumpled, corroded and degraded (Tipping, 1987; McCulloch and Davies, 2001; Mansilla et al., 2018). Pollen grains are best preserved (i.e. normal) in wetter-acidic and anaerobic conditions found in low-energy environments such as peat bogs and undisturbed lake sediments. Broken and crumpled pollen may reflect a more abrasive and/or energetic environment prior to final deposition. Corroded and degraded pollen are considered to have been damaged by oxidation and the actions of bacteria and fungi (biochemical factors) operating under more aerobic conditions.

3. Results

3.1. Sediment stratigraphy

A simplified stratigraphy of the core from Cta. Euegnia is shown alongside the LOI_{550} profile in Figure 3. From 900 cm to 882 cm, the basal sediments comprise compact light bluish-grey clays and silts and were probably deposited under a proglacial lake following glacier retreat. Between 882 cm and 838 cm the sediment gradually increases in organic content to form a rich lacustrine mud but with sub-centimetre bands of bluish-grey clays suggesting the warming trend was punctuated by brief reversals. At 842 cm the lacustrine mud is overlain by a 28 cm thick layer of soft bluish-grey clays. The clays are dissimilar in colour and degree of compactness in comparison to the basal clays and silts and we suggest they are periglacial solifluction clays rather than a return to direct glacial inputs to the site. Overlying the clays is a 10 cm layer of organic rich lacustrine mud which grades rapidly into compact well-humified peat to 764 cm. Between 764 cm and 746 cm there is a brief increase in mineral content before returning to peat. The accumulation of peat continues to 636 cm where it is truncated by a sharp contact to greenish-grey clays and silts with occasional fragments of mollusc shells suggesting the sediments are marine in origin. The sharp contact between the peat and the overlying marine sediments may represent an erosive contact. However, we suggest it is unlikely as the marine sediments are clay-silts indicative of a low-energy depositional environment. Relatively homogenous marine sediments continue to accumulate until ~431 cm when the stratigraphy becomes more banded and small peaks in organic content occur. From 409 cm the stratigraphy gradually develops into an organic rich fine lacustrine mud / fen peat (>80%) which continues to 360 cm above which it becomes a very pale brown, very fibrous peat. Between 288 cm and the surface the peat accumulation continues with varying degrees of fibrous content and compactness.

Light and polarised light microscopy analysis of the mineral residue from the LOI_{550} samples identified two cryptotephra layers: Mount Burney (~52°S), a white silt layer at 236 cm (MB2) and Volcán Hudson (~46°S), a dark olive-green coarse silt layer at 612 cm (H1). The glass component of each tephra layer was isolated using the preparation methodology of Dugmore et al. (1992). Individual glass shards were geochemically analysed by RMcC using an SX100 Cameca Electron Microprobe at the School of GeoSciences, The University of Edinburgh (Hayward, 2011). The ages for each geochemically identified tephra layer are included in Table S1.

3.2. Chronology

The core is constrained by 8 AMS radiocarbon dates on bulk organic material and from fine plant material. The ^{14}C minimum and maximum ages for the period of marine sedimentation were obtained from millimetre slices of peat / organic rich lacustrine mud immediately below and above the marine clays respectively. Therefore, we are confident that any marine reservoir effect will be negligible. Ages for the H1 and MB2 tephras were also included to provide a more robust chronology (Table 1). The Bayesian modelling software BACON (Blaauw and Christen, 2011) was used to construct the age–depth model (Fig. 3). The weighted mean ages from the BACON age–depth model were used to provide the age–depth axis (cal a BP) for the pollen diagrams: percentage pollen (Fig. 4), pollen accumulation rate (influx) (Fig. 5) and percentage pollen preservation (Fig. 6).

3.3. Palaeoenvironmental results and inferences

Seven Local Pollen Assemblage Zones (LPAZs) were defined for the Cta. Eugenia pollen record using constrained cluster analysis and applied to Figs. 4, 5 and 6 to aid comparison.

3.3.1. LPAZ CE-1 (882–842 cm; 16,290 – 15,470 cal a BP)

The basal LPAZ is dominated by fluctuating amounts of relatively poorly preserved (Normal = ~30-40%) *Gunnera* and *Empetrum rubrum*. The organic content gradually increases starting from the sterile bluish-grey clays at the base and there is a small amount of Cyperaceae (~10-20%), though aquatic pollen are absent. This suggests that the basin was occupied by open water ringed by sedges and the recently deglaciated terrain and development of soils surrounding the site was initially colonised by *Gunnera* ground cover and *Empetrum* heath, shifting in response to small-scale changes in effective moisture. Although the trend is towards more temperate conditions, climate continues to be cool and favours cold-tolerant taxa. The warming trend is then interrupted at c. 15,470 cal a BP indicated by the deposition of barren periglacial bluish-grey clays which continues until c. 14,530 cal a BP.

3.3.2. LPAZ CE-2 (814–754 cm; 14,530 – 12,390 cal a BP)

After the cessation of clay accumulation, the pollen assemblage dramatically changes to be dominated by Poaceae with lesser amounts of *Empetrum rubrum* and *Caltha*. This suggests a shift to a drier landscape largely covered by grasses surrounding the site and the water level at the site shallowing in response to drier conditions leading it to be dominated by Cyperaceae (>60%) and *Caltha*. This picture is reinforced by the continued poor preservation of the terrestrial pollen (Normal = ~30%), the compact and dark fine-detrital sediment and the slower rate of sediment accumulation (~35 a cm^{-1}). The small increase in the influx of Cyperaceae suggests the extent of open water was reduced and sedges were able to spread across the site.

3.3.3. LPAZ CE-3 (754–632 cm; 12,390 – 8540 cal a BP)

This LPAZ marks the continuous deposition of *Nothofagus dombeyi* type pollen (>2%) which probably reflects the dispersal of southern beech trees into the area in response to ameliorating climatic conditions, although the pollen influx of *Nothofagus dombeyi* type remains very low. The establishment of *Nothofagus* forest (~20% TLP; 'Parque' *sensu* Burry et al., 2006) occurs later at c. 10,640 cal a BP and this is mirrored by the coeval increase in the hemiparasite *Misodendrum* that favours *Nothofagus antarctica* and *Nothofagus pumilio*. However, the expansion of the forest was likely constrained by the continued relatively drier conditions evidenced by the increase in corroded and degraded pollen (Normal = ~10-20%) and the proportion of *Nothofagus dombeyi* type declines towards the upper boundary. This constraint is reflected in the continued dominance of steppe vegetation (Poaceae, subf. Asteroideae) which replaced Cyperaceae across the drier site and the rate of sediment accumulation slowed to its lowest level (~48 a cm^{-1}) of the whole record. A shift to warmer drier conditions is also emphasised by the dramatic expansion in Polypod ferns (Polypodiaceae) and the increase in charcoal influx, probably as a result of the increase in the availability of drier fuel.

3.3.4. LPAZ CE-4 (632–408 cm; 8540 - 6680 cal a BP)

This LPAZ marks the very rapid relative sea-level rise and inundation of the mire at Cta. Eugenia. The stratigraphic transition occurs at c. 8640 cal a BP (636 cm) from peat to greenish-grey clays and silts within <10 years. The rapid and categorical change in stratigraphy is also reflected in the increase in *Nothofagus dombeyi* type pollen and improvement in pollen preservation (Normal ~65%), a corresponding decrease in steppe vegetation (Poaceae, subf. Asteroideae) and the gradual decline in Polypod ferns which began towards the top of LPAZ CE-3. Climatic inferences from this LPAZ are limited as it is unlikely that forest expansion and increase in humidity was synchronous with the sea level rise. It is probable that that the marine inundation resulted in the over-representation of *Nothofagus*, a prolific producer of pollen, against a backdrop of low pollen influx. The dominance of *Nothofagus* pollen within a range of ecological settings, from montane to lowland environments, is demonstrated by sampling of the modern pollen rain in the region (Heusser, 1989). However, the richness of the coastal flora is still represented by the persistence of trace amounts of *Acaena*, subf. Asteroideae, Caryophyllaceae, *Plantago* and *Gunnera*.

3.3.5. LPAZ CE-5 (408-248 cm; 6680 - 4310 cal a BP)

LPAZ CE-5 is divided into three sub-zones that reflect the gradual emergence of the site as relative sea-level lowered. The basin morphology of the site has been maintained by the formation of a series of storm beach ridges reaching ~4.0 m a.s.l. (Fig. 2). The storm beach ridges have both protected the soft-sediments at the site from coastal erosion and enabled the development of an isolated freshwater lagoon and this is reflected in the increasing organic-rich stratigraphy and expansion of freshwater taxa during LPAZ CE-5a. The transition from marine sediments to the organic rich freshwater sediments occurs over ~420 years. However, there are two peaks in *Hippuris vulgaris* and *Myriophyllum* at c. 6600 and 5690 cal a BP separated by a peak in freshwater algae, a brief increase in mineral content and near absence of charcoal. These changes probably indicate that the initial trend to shallower water indicated by the change from *Myriophyllum* to Poaceae-*Caltha* wet meadow was interupputed by a pluvial period that led to clear still and deeper water at the site and a reduction in the availability of drier fuel.

LPAZ CE-5b (c. 5780 cal a BP) marks the restart of the hydroseral succession and the return of shallower water conditions, a brief expansion of *Hippuris vulgaris* and *Myriophyllum* and then continued drying at the surface of the site facilitating the growth of Poaceae. *Nothofagus* proportions reach their lowest values (~20%) since the Late glacial – early Holocene transition. This decline in *Nothofagus* commenced in LPAZ CE-5a and the initial decline probably reflects the changing balance of pollen inputs following the end of the marine environment. However, the continued contraction of *Nothofagus* cover during LPAZ CE-5b, also suggested by the reduction in *Nothofagus* influx, was probably a response to a shift to drier climatic conditions. This inference is reinforced by the steady increase in corroded and degraded pollen (Normal declines from ~80% to ~25%) and a small increase in charcoal at the same time. During LPAZ CE-5c there is a rapid shift to wetter conditions indicated by the reduction in Poaceae and a shift to heath vegetation and a dramatic improvement in the preservation of pollen (Normal = ~60%). The increase in effective moisture also facilitated an expansion of *Nothofagus* woodland (~50%).

3.3.6. LPAZ CE-6 (248-136 cm; 4310-2180 cal a BP)

The heath vegetation that developed during the preceding LPAZ was rapidly replaced by *Nothofagus* woodland. At c. 4160 cal a BP (236 cm) the MB2 cryptotephra was deposited. A small and brief peak in Poaceae occurs at the time of the deposition of the tephra layers but the expansion of *Nothofagus,* also reflected in a large peak in pollen influx values, commenced ~200 years prior to the eruption. Between c. 4310 and 3220 cal a BP the woodland appears to be open and *Misodendrum* and Polypod ferns also flourished. *Nothofagus* wood fragments can be found in the core during this period indicating the expansion of *Nothofagus* over the mire surface. The evidence suggests that there was a rapid change from the wetter conditions of LPAZ-5c to drier climatic conditions that led to a significant reduction in mire surface wetness (MSW). This sustained period of dryness led to the decline of the *Empetrum* heathland and the expansion of *Nothofagus* woodland onto the mire surface between c. 4310 and 3220 cal a BP. This climatic inference is further supported by the dramatic increase in corroded and degraded pollen (Normal = ~20%). The expansion of *Nothofagus* covering the mire increased the local input of *Nothofagus dombey*i type pollen during this LPAZ which gives the appearance of the dominance of woodland. However, the mire pollen input masks the pollen signal from the surrounding landscape at this time. It is likely that the surrounding *Nothofagus* woodland would have been more open under such drier climatic conditions and that the mire formed an oasis of woodland cover.

At c. 3220 cal a BP the forest became more closed (*Nothofagus* ~90%) and *Misodendrum* and virtually all other taxa were excluded from the record. There is also an increase in normally preserved pollen from which an increase in humidity and MSW is inferred. The trend to wetter conditions is interrupted at c. 2390 - 1830 cal a BP by a brief return to drier conditions, as evidenced by an increase in corroded and degraded pollen and a large peak of charcoal at c. 2550 cal a BP.

3.3.7. LPAZ CE-7 (136cm-surface; 2180 - present cal a BP)

During LPAZ CE-7 the general trend to wetter conditions that commenced at c. 3000 cal a BP continues leading to an increase in MSW inferred from improved pollen preservation and the return of *Empetrum* heathland. The decline of *Nothofagus* appears to be at odds with the inferred increase in humidity. However, we argue that the contraction of woodland should be viewed in the context of the preceding LPAZ CE-6 and the reduction in *Nothofagus* probably reflects the loss of trees from the wetter mire surface and a rebalancing of pollen inputs. Between c. 2180 and present *Nothofagus* proportions fluctuate around ~60% of TLP and trace amounts of *Drimys winteri* also suggest increasing plant diversity within a more open forest canopy. The site continued to experience periods of rapid climate change as the general trend to increased MSW was punctuated by short but high magnitude periods of drier climate inferred from fluctuations between heath and woodland. Reductions in normally preserved pollen and coupled with peaks in charcoal occurred at c. 1830 cal a BP, 1160 cal a BP, 500 cal a BP. The final peak in charcoal <100 years ago was probably due to woodland clearance of the coastal margin of Isla Navarino by European settlers.

4. Discussion

4.1. Climatic inferences from the Cta. Eugenia record

The basal minimum age for deglaciation at Cta. Eugenia suggests the Canal Beagle glacier had retreated from its eastern LGM extent some time before c.16,200 cal a BP. Age constraints for the LGM in the Canal Beagle are limited but the minimum age from Cta. Eugenia is almost certainly an underestimate as it is likely that ice retreat began at least ~1000 years earlier but the persistence of periglacial tundra inhibited the growth and accumulation of dateable organic material at the site. The onset of relatively warmer and more humid conditions is indicated by the initial heath and *Gunnera* assemblage, however, the treeless landscape suggests the persistence of colder conditions in comparison to later Holocene interglacial conditions. This picture is similar to the nearest Late glacial record from Pto. Harberton which commenced at c. 16,000 cal a BP and was also initially colonised by heath and *Gunnera* vegetation (Markgraf, 1993). However, at Cta. Eugenia the trend to slightly warmer conditions was interrupted by the deposition of soliflucted clays between c. 15,470 and 14,530 cal a BP. The timing of this 'cooling' event does not correlate to the onset of the Antarctic Cold Reversal (ACR, c. 14,440 – 12, 760 cal a BP) (Gest et al., 2017) and is not identified in any of the other records from around the Canal Beagle and so for the moment this event appears to be site-specific. Somewhat counter intuitively at c. 14,530 cal a BP the stratigraphic evidence suggests relatively warmer conditions resumed which continued during the ACR. However, the pollen assemblage, and in particular the poor pollen preservation, continues to reflect the persistence of colder and drier conditions relative to the present interglacial. The identification of a cooling event equivalent to the ACR in southern Patagonia is challenging as steppe-tundra vegetation is cold-tolerant and so not necessarily sensitive to the relatively small-scale cooling as indicated by Antarctic ice cores during the ACR (Jouzel et al., 2007). However, the southern Patagonian Late glacial vegetation is responsive to latitudinal shifts in the belt of precipitation driven by the southern westerly winds (SWWs). It is probable that Antarctic cooling during the ACR impeded and / or reversed the southerly migration of the SWWs following deglaciation after the LGM (Hulton et al., 2002; Lamy et al., 2010) leading to the drier conditions at Cta. Eugenia between c. 14,530 and 12,390 cal a BP.

The glacial-interglacial transition was a gradual process of warming indicated by the arrival of *Nothofagus* woodland in the area commencing at c. 12,390 cal a BP. This is close to the age for woodland expansion at Pto. Harberton at c. 12,200 cal a BP (Markgraf and Huber 2010). The arrival of *Nothofagus* appears to be earlier at the eastern end of Canal Beagle than at other sites in the region that suggest ages closer to c. 10,500 cal a BP (Mansilla et al., 2018). However, the difference probably reflects the closer proximity of Cta. Eugenia and Pto. Harberton to woodland refugia during the last glaciation on Peninsula Mitre (Premoli et al., 2010; Mansilla et al., 2016) and that the other sites are either more montane or closer to the Cordillera Darwin ice field and so deglaciated later. The establishment of *Nothofagus* woodland at Cta Eugenia occurred at c. 10,640 cal a BP which is closer to the timing of the regional expansion of *Nothofagus* woodland and marks the onset of warmer Holocene conditions.

The limited expansion of the *Nothofagus* woodland and indications of declining humidity as temperatures increased after c. 12,390 cal a BP contrasts with the evidence for greater humidity at ~52-53°S (McCulloch and Davies, 2001; Markgraf and Huber, 2010; Mansilla et al., 2016; 2018). This suggests that the SWWs may have been more focussed to the north of the Cordillera Darwin divide at this time. However, after c. 11,000 cal a BP there is widespread regional drier conditions leading to the westward contraction of the *Nothofagus* forest ecotone and increased fire frequency between 52° and 55°S. This period of regional dryness is contemporary with the thermal maximum of sea surface temperatures (SSTs) at ~53°S (Lamy et al., 2010). We suggest the increased temperatures and a more southerly focus of the SWWs led to drier conditions at Cta. Eugenia and increased ocean temperatures along the western margins of the Antarctic Pensinsula and the eventual loss of ice shelves (Bentley et al., 2009). The period of relative dryness continues at Cta. Euegnia until the climatic record is interrupted by the mid-Holocene marine incursion at c. 8640 cal a BP. Previous studies of marine transgression sediments have suggested that the *Nothofagus* forest dominated the landscape at this time (Borromei and Quattrocchio, 2007). However, the *Nothofagus* influx values at Cta. Eugenia do not support the near-closed forest indicated by the percentage pollen data, which is more an artefact of the change of balance between the different pollen sources to the basin. We suggest estimations of woodland cover based on percentage data alone from marine or lacustrine sites should be treated with caution.

Following relative sea-level lowering at c. 6690 cal a BP the lagoon at Cta. Eugenia followed the natural hydroseral process of basin infilling and vegetation development leading to the re-establishment of a mire. Climatic inferences from this period are limited but the interruption of the shallowing of the lagoon during LPAZ CE-5a suggests a pluvial period at c. 6000 cal a BP. Along the Canal Beagle this wetter period is broadly contemporary with an increase in aquatic and wetland taxa at Pta. Moat and more humid conditions and reduced fire activity at Pto. Harberton (Markgraf and Huber, 2010). This period may mark the return of the SWWs closer to their present focus in response to reduced SSTs and cooler climate (Lamy et al., 2010).

Between 5550 and 4830 cal a BP a gradual shift to drier conditions at Cta. Eugenia leads to a contraction of the forest margin and expansion of steppe vegetation. However, this is not evident in other records from along the Canal Beagle. In contrast, sites to the north of the Canal Beagle and Cordillera Darwin suggest a shift to wetter conditions leading to the development of closed-canopy *Nothofagus* woodland and a decline in fire frequency (Markgraf and Huber, 2010; Ponce and Fernandez, 2014; Musotto et al., 2016; Mansilla et al., 2018). This north-south divide in the climatic signals suggests the core of the SWWs was probably focused more to the north of ~54°S.

After c. 4780 cal a BP the Cta. Eugenia record suggests a marked increase in wetter conditions and this is similarly reflected in the expansion and persistence of dense closed-canopy *Nothofagus* forest across the region (Markgraf and Huber, 2010; Ponce and Fernandez, 2014; Musotto et al., 2016; Mansilla et al., 2018). However, this increase in humidity at Cta. Eugenia is relatively short and at c. 4310 cal a BP there was a marked reversal to drier conditions that persisted until c. 3220 cal a BP. However, the pollen records from Pto. Harberton and Cta. Lacroix display minimal fluctuations in the *Nothofagus* cover between c. 5500 cal a BP and c. 1000 which suggests a degree of insensitivity. It is probable that the Cta. Lacroix record also reflects South Atlantic moisture sources during periods of less intense SWWs. Sites to the north of the Cordillera Darwin suggest the continued dominance of *Nothofagus* forest but the record at Lago Lynch does indicate a westward contraction of the forest-steppe ecotone and increase in fire activity just after the eruption of Mt. Burney (MB2) (Mansilla et al., 2018).

From c. 3220 cal a BP to the present there was a general trend to increasing wetness at Cta. Eugenia and this is also reflected in records from across the region evidenced by the continued dominance of *Nothofagus* forest and the gradual expansion of heath bog communities (Markgraf and Huber, 2010; Mansilla et al., 2016). However, the trend to wetter conditions is punctuated by several short periods of rapid climate change leading to drier intervals at c. 2390-1830 cal a BP, 1160 cal a BP and 500 cal a BP. and we argue that the drier periods at Cta. Eugenia represent warmer periods when the SWWs were driven more polewards. The evidence for the sequence of drier intervals between c. 4300 and 500 cal BP suggests the geographical location of Cta. Eugenia and its mire hydrology render it acutely sensitive to latitudinal shifts in the moisture bearing SWWs.

4.2. Mid-Holocene marine incursion and implications for the human record

The mid-Holocene marine incursion at Cta. Eugenia occurred at c. 8640 cal a BP and the contact between the underlying peat and the marine sediments indicates a sub-millimetre boundary to deeper water clays which, within the constraints of the age-depth model, suggests the transition took place over less than tens of years. At present there are no estimates of the rate of isostatic rebound in the region but the inundation at Cta. Eugenia appears to have been rapid at a time when global sea level rise was also rapid (Fleming et al., 1998). Holocene neotectonic displacement of palaeoshorelines has been identified along the South American – Scotia plate boundary (McCulloch and Bentley, 2005) and discordant data has been obtained from marine transgression sites along the Canal Beagle (Borromei and Quattrocchio, 2007). However, the mid-Holocene marine transgression shoreline is a consistent feature along much of the north shore of Isla Navarino and indicates the spatial extent of the changing nature of the coastline that probably affected early humans living along the Canal Beagle.

Archaeological evidence in the form of abundant shell middens, usually located within embayments along the shore of Isla Navarino, suggest a close association between human activity and proximity to the shoreline. The arrival of early people has been estimated at c. 8700 to 8400 cal a BP (Zangrando et al., 2019) in the Canal Beagle but evidence for earlier presence of human populations has potentially been lost during the transgressive phase of the marine incursion between c. 8640 and 6690 cal a BP. Continued isostatic uplift resulted in coastal emergence, relative sea level lowering and the isolation of the basin at Cta. Eugenia. This pattern is tentatively reflected in the spatial and temporal distribution of shell middens and other domestic archaeological assemblages recently excavated by the authors at Bahia Mejíllones on the north shore of Isla Navarino. The oldest shell midden layer is dated to c. 6890 cal a BP and is located at ~7.5 m a.s.l., while the age distribution of the lower shell middens declines with altitude and increasing proximity to the present shoreline (San Roman et al., 2017).

5. Conclusions

The palaeoenvironmental evidence from Cta. Eugenia provides new insights into the sequence of environmental and climatic changes that have driven landscape evolution along the north shore of Isla Navarino and the Canal Beagle. After deglaciation at c. 16,200 cal a BP cooler climatic conditions persisted until gradual warming led to the establishment and expansion of *Nothofagus* forest between c. 12,390 and c.10,640 cal a BP. However, during the early to mid-Holocene we argue for increased temperatures and / or a poleward intensification of the SWWs leading to drier conditions in Fuego-Patagonia. The rapid inundation of Cta. Eugenia by the mid-Holocene marine transgression interrupts the climate signal from the site but offers additional insights into the timing and nature of changes that impacted on the coastal landscape and availability of resources to early humans along the north coast of Isla Navarino. The emergence of the site following relative sea-level lowering at c. 6690 cal a BP re-establishes the climatic record from Cta. Eugenia. After c. 4780 cal a BP there is trend to increasing MSW which is punctuated by several periods of rapid climate change which produced drier conditions (c. 4310 to c. 3220 cal a BP; c. 2390-1830 cal a BP, 1160 cal a BP and 500 cal a BP). The intervening wetter periods recorded at Cta. Eugenia probably reflect a more equatorward latitudinal position of the SWWs during relatively cooler periods. We suggest the geographical position of Cta. Eugenia, to the south-east of the Cordillera Darwin divide has rendered the site sensitive to latitudinal shifts in the SWWs along the west coast of southern Patagonia and the Antarctic Peninsula. The sensitivity of Cta. Eugenia is also reinforced by the application of multiple lines of evidence from the pollen record; sediment stratigraphy, percentage pollen, pollen influx and particularly pollen preservation, which combined support robust climatic and ecological inferences.

Acknowledgements

RMcC is supported by 'Programa Regional CONICYT R17A10002'. Field work and analyses by RMcC, FM and MSR were supported by 'FONDECYT 1140939'; CAM was supported by FONDECYT 3180280 and CONICYT PAI/SIA conv. 2018, N77180002. The Tephra Analytical Unit, School of GeoSciences, The University of Edinburgh, provided support for the Electron Microprobe analyses of tephra samples by RMcC. We thank Dr Mary McCulloch and Subrina Murray for their assistance in the field. RMcC is particularly grateful to Mr Andrew Moss, University of Birmingham, for his patient mentoring in the art of Pollen Analysis. We are very grateful to Prof. Vera Markgraf and an anonymous reviewer for their constructive comments on an earlier version of the manuscript.

References

Bentley, M.J. and McCulloch, R.D. 2005: Impact of neotectonics on the record of glacier and sea level fluctuations, Strait of Magellan, southern Chile. Geografiska Annaler, 87 A(2): 393–402.

Bentley, M.J., Hodgson, D.A., Smith, J.A., Cofaigh, C.Ó., Domack, E.W., Larter, R.D., Roberts, S.J., Brachfeld, S., Leventer, A., Hjort, C., Hillenbrand, C.D., Evans, J., 2009. Mechanisms of Holocene palaeoenvironmental change in the Antarctic Peninsula region. The Holocene, 19: 51–69.

Blaauw, M., Christen, J.A., 2011. Flexible paleoclimate age-depth models using an autoregressive gamma process. Bayesian Analysis, 6: 457–474.

Borromei, A.M. 1995. Análisis polínico de una turbera holocénica en el Valle de Andorra, Tierra del Fuego, Argentina. Revista Chilena de Historia Natural, 68: 311-319.

Borromei, A.M. and Quattrocchio, M. 2007. Holocene sea-level change inferred from palynological data in the Beagle Channel, southern Tierra del Fuego, Argentina. Revista de la Asociación Geológica Argentina, 44(1): 161-171.

Borromei, A.M., Ponce, J.F., Coronato, A., Candel, M.S., Olivera, D., Okuda, M. 2014. Reconstrucción de la vegetación posglacial y su relación con el ascenso relativo del nivel del mar en el extremo este del canal Beagle, Tierra del Fuego, Argentina. Andean Geology, 41(2): 362-379.

Bujalesky, G. 2011. The flood of the Beagle Valley (11,000 yr B.P.) Tierra del Fuego. Anales del Instituto Patagonia, 39(1): 5-21.

Burry, L.S., Trivi de Mandri, M., D'Antoni, H.L., 2006. Paleocomunidades vegetales del centro de Tierra del Fuego durante el Holoceno temprano y tardío. Revista del Museo Argentino de Ciencias Naturales, 8: 127–133.

Candel, M.S., Martínez, A.M., Borromei, A.M. 2011. Palinología y palinofacies de una secuencia marina del Holoceno medio-tardío: albufera lanushuaia, canal beagle, Tierra del Fuego, Argentina. Revista Brasileira de Paleontologia, 14(3): 297-310.

Dugmore, A.J., Larsen, G., Newton, A.J., Sugden, D.E., 1992. Geochemical stability of fine-grained silicic tephra layers in Iceland and Scotland. Journal of Quaternary Science, 7: 173–183.

Fleming, K., Johnston, P., Zwartz, D., Yokoyama, Y., Lambeck, K., Chappell, J. 1998. Refining the eustatic sea-level curve since the Last Glacial Maximum using far- and intermediate-field sites. Earth and Planetary Science Letters, 163(1-4): 327-342.

Gest, L., Parrenin, F., Chowdhry Beeman, J., Raynaud, D., Fudge, T.J., Buizert, C., Brook, E.J. 2017. Leads and lags between Antarctic temperature and carbon dioxide during the last deglaciation. Climate of the Past Discussions, doi:10.5194/cp-2017-71.

Grill, S., Borromei, A.M., Quattrocchio, M., Coronato, A., Bujalesky, G., Rabassa, J. 2002. Palynological and sedimentological analysis of Recent sediments from Río Varela, Beagle Channel, Tierra del Fuego, Argentina. Revista Española de Micropaleontología, 34: 145-161.

Grimm, E.C., 1987. CONISS; a FORTRAN 77 program for stratigraphically constrained cluster analysis by the method of incremental sum of squares. Computers in Geosciences, 13(1): 13–35.

Grimm, E.C., 2011. Tilia and Tiliagraph. Illinois State Museum, Illinois.

Hall, B. L., Denton, G., Lowell, T., Bromley, G. R. M., Putnam A. E. 2018. Retreat of the Cordillera Darwin icefield during Termination I. Cuadernos de Investigación Geográfica, 43(2): 751-766.

Hayward, C., 2011. High spatial resolution electron probe microanalysis of tephras and melt inclusions without beam-induced chemical modification. The Holocene, 22: 119–125.

Heusser, C.J., 1971. Pollen and Spores of Chile. The University of Arizona Press, Tucson, Arizona (167 pp.).

Heusser, C.J., 1989. Late Quaternary vegetation and climate of southern Tierra del Fuego. Quaternary Research, 31: 396–406.

Heusser, C.J. 1998. Deglacial paleoclimate of the American sector of the Southern Ocean: Late Glacial-Holocene records from the latitude of Canal Beagle (55°S), Argentine Tierra del Fuego. Palaeogeography, Palaeoclimatology, Palaeoecology, 141: 277-301.

Hogg, A.G., Hua, Q., Blackwell, P.G., Niu, M., Buck, C.E., Guilderson, T.P., Heaton, T.J., Palmer, J.G., Reimer, P.J., Reimer, R.W., Turney, C.S.M., Zimmerman, S.R.H., 2013. SHCal13 southern hemisphere calibration, 0–50,000 years cal BP. Radiocarbon, 55: 1889–1903.

Jouzel, J., Masson-Delmotte, V., Cattani, O., Dreyfus, G., Falourd, S.; Hoffmann, G., Minster, B., Nouet, J., Barnola, J., Chappellaz, J., Fischer, H., Gallet, J. C., Johnsen, S., Leuenberger, M., Loulergue, L., Luethi, D., Oerter, H., Parrenin, F., Raisbeck, G., Raynaud, D., Schilt, A., Schwander, J., Selmo, E., Souchez, R., Spahni, R., Stauffer, B., Steffensen, J.P., Stenni, B., Stocker, T., Tison, J-L., Werner, M., Wolff, E.W. (2007). Orbital and millennial Antarctic climate variability over the past 800,000 years. Science, 317(5839): 793-797.

568 Jowsey, P.C., 1966. An improved peat sampler. New Phytologist, 65: 245–248.

569

570 Lamy, F., Kilian, R., Arz, H.W., Francois, J-P., Kaiser, J., Prange, M., Steinke, T. 2010. Holocene changes in
571 the position and intensity of the southern westerly wind belt. Nature Geoscience, 3: 695-699.

572

573 Legoupil, D., 1993. El Archipiélago del Cabo de Hornos y la Costa Sur de la Isla Navarino: Poblamiento y
574 Modelo Económicos. Anales del Instituto de la Patagonia, Serie Cs. Humanas 22: 101–122.

575

576 Massone, M., 2004. Los cazadores después del hielo, Colección de Antropología VII. Dirección de
577 Bibliotecas, Archivos y Museos, Santiago.

578

579 Mansilla, C.A., McCulloch, R.D., Morello, F., 2016. Palaeoenvironmental change in southern Patagonia
580 during the Lateglacial and Holocene: implications for forest refugia and climate reconstructions.
581 Palaeogeography, Palaeoclimatology, Palaeoecology, 447: 1–11

582

583 Mansilla, C.A., McCulloch, R.D. Morello, F. 2018. The vulnerability of the Nothofagus forest-steppe
584 ecotone to climate change: Palaeoecological evidence from Tierra del Fuego (~53°S). Palaeogeography,
585 Palaeoclimatology, Palaeoecology, 508: 59-70.

586

587 Markgraf, V., 1993. Paleoenvironments and paleoclimates in Tierra del Fuego and southernmost
588 Patagonia, South America. Palaeogeography, Palaeoclimatology, Palaeoecology, 102: 351–355.

589

590 Markgraf, V., Huber, U.M., 2010. Late and postglacial vegetation and fire history in southern Patagonia
591 and Tierra del Fuego. Palaeogeography, Palaeoclimatology, Palaeoecology, 297 (2): 351–366.

Martin, F., 2006. Carnívoros y huesos humanos de Fuego-Patagonia. Aportes desde la tafonomía forense. Colección Tesis de Licenciatura. Sociedad Argentina de Antropología, Buenos Aires.

McCulloch, R.D., Davies, S.J., 2001. Late-glacial and Holocene palaeoenvironmental change in the Central Strait of Magellan, Southern Patagonia. Palaeogeography, Palaeoclimatology, Palaeoecology, 173: 143–173.

McCulloch, R., Fogwill, C., Sugden, D., Bentley, M., Kubik, P., 2005. Chronology of the last glaciation in central Strait of Magellan and Bahía Inútil, southernmost South America. Geografiska Annaler, Ser. B 87 (2): 289–312.

McCulloch, R., Morello, F., 2009. Evidencia glacial y paleoecológica de ambientes tardiglaciales y del Holoceno temprano. Implicaciones para el Poblamiento Temprano de Tierra del Fuego, in: Salemme, M., Santiago, F., Álvarez, M., Piana, E., Vázquez, M., Mansur, M.E. (Eds.), Arqueología de Patagonia: Una Mirada Desde El Último Confín. Editorial Utopías, Ushuaia, pp. 119–136.

Moore, P.D.,Webb, J.A., Collinson, M.E., 1991. Pollen Analysis. Blackwell Scientific, London (216 p.).

Musotto, L.L., Borromei, A.M., Bianchinotti, M.V., Coronato, A., Menounos, B., Osborn, G., Marr, R., 2016. Postglacial environments in the southern coast of Lago Fagnano, central Tierra del Fuego, Argentina, based on pollen and fungal microfossils analyses. Review of Palaeobotony and Palynology, 238: 43–54.

616 Ocampo, C., Rivas, P., 2000. Nuevos fechados 14C de la costa norte de la isla Navarino, costa sur del canal Beagle, Provincia Antarctica Chilena, Región de Magallanes. Anales del Instituto de la Patagonia, Serie Ciencias Humanas, 28: 197–214.

620 Orquera, L.A., Piana, E.L., 2009. Sea Nomads of the Beagle Channel in Southernmost South America: Over Six Thousand Years of Coastal Adaptation and Stability. The Journal of Island and Coastal Archaeology, 4: 61–81.

624 Pisano, E. 1994. Sectorización fitogeográfica del archipiélago sud patagónico-fueguino: Sintaxonomía y distribución de las unidades de vegetación vascular. Anales del Instituto de la Patagonia, Serie Ciencias Naturales, 21: 5-33.

628 Ponce, J. F., Fernandez, M. 2013. Climatic and Environmental History of Isla de los Estados, Argentina. Editorial Springer, Dordrecht (128 p.).

631 Premoli, A., Mathiasen, P., Kitzberger, T., 2010. Southern-most *Nothofagus* trees enduring ice ages: genetic evidence and ecological niche retrodiction reveal high latitude (54°S) glacial refugia. Palaeogeography, Palaeoclimatology, Palaeoecology, 298: 247–256.

635 Rabassa, J.; Coronato, A.; Bujalesky, G.; Salemme, M.; Roig, C.; Meglioli, A.; Heusser, J.; Gordillo, S.; Roig, F.; Borromei, A.; Quattrocchio, M. 2000. Quaternary of Tierra del Fuego, Southernmost South America: an updated review. Quaternary International, 68-71: 217-240.

Rozzi, R., 2012. Filosofía ambiental sudamericana: raíces amerindias ancestrales y ramas académicas emergentes. Environmental Ethics, 34: 9–32.

San Román, M. (2018). Los arpones y armas de hueso de las colecciones del Museo Antropológico Martin Gusinde: Tecnología emblemática de la interacción entre humanos y el mar en el confín de América. Colecciones Digitales, Subdirección de Investigación Dibam.

San Roman, M., Sierpe, V., Torres, J., Martinez, I., Palacios, C., Mardones, J., Barrientos, M.J., Christensen, M., Borrero, L., Massone, M., Martin, F., Rodriguez, K., Morello, F., 2017. New information of marine hunter-gatherers of the Southernmost End of South America: technological and zooarchaeological study of site Bahía Mejíllones 45 (6850 Cal BP), northern coast of Navarino Island, 55° South Latitude, Chile, in: 82nd Annual Meeting of the Society for American Archaeology, Vancouver, BC, Canada.

Stern, C.R., Moreno, P.I., Henriquez, W.I., Villa-Martinez, R., Sagredo, E., Aravena, J.C., De Pol-Holz, R., 2016. Holocene tephrochronology around Cochrane (~47°S), southern Chile. Andean Geology, 43(1): 1–19.

Stockmarr, J., 1971. Tablets with spores used in absolute pollen analysis. Pollen et Spores, 13: 615–621.

Stuiver, M., Reimer, P.J. 1993. Extended ^{14}C database and revised CALIB radiocarbon calibration program. Radiocarbon, 35: 215-230.

Tipping, R., 1987. The origins of corroded pollen grains at five early postglacial pollen sites in Western Scotland. Review of Palaeobotony and Palynology, 53: 151–161

Troels-Smith, J. 1955. Characterization of unconsolidated sediments. Danmarks Geologiske Undersøgelse, Series IV, 3: 38-73.

Tuhkanen, S., Kuokka, I., Hyvönen, J., Stenroos, S., Niemela, J., 1989–1990. Tierra del Fuego as a target for biogeographical research in the past and present. Anales del Instituto Patagonia, 19: 5–107.

Whitlock, C., Larsen, C., 2001. Charcoal as a fire proxy. In: Last, W.M., Smol, J.P. (Eds.), Tracking Environmental Change Using Lake Sediments. Vol. 3, Terrestrial, Algal and Siliceous Indicators Kluwer Academic Publishers, Dordrecht (371 p.).

Wingenroth, M., Heusser, C.J., 1984. Pollen of the High Andean Flora. Quebrada Benjamin Matienzo, Province of Mendoza Argentina. Mendoza: Instituto Argentino de Nivologia y Glaciologia, Mendoza (195 p.).

Zangrando, A.F., Bjerck, H.B., Piana, E.L., Breivik, H.M., Tivoli, A.M., Negre, J., 2018. Spatial patterning and occupation dynamics during the Early Holocene in an archaeological site from the south coast of Tierra del Fuego: Binushmuka I. Eestudios Atacameños, Arqueología y Antropología Surandinas, 60: 31–49.

Table 1

Laboratory Code	Depth (cm)	Material	^{14}C yr (1σ)	$\delta^{13}C$ ‰	Calibrated age range (95.4%) cal. yr BP†	Calibrated age range (WMA) (95%) cal. yr BP‡
UGAMS38371	140	Bulk peat	2260 ± 20	-26.7	2156 - 2320	2161 – (2248) - 2339
Tephra MB2 [1]	236	-	3860 ± 50	-	4013 - 4413	3905 – (4151) - 4375
UGAMS38372	342	Bulk peat	4710 ± 20	-32.0	5315 - 5566	5328 – (5437) - 5583
UCIAMS189842	409	Bulk lacustrine mud	5970 ± 20	na	6670 - 6843	6472 – (6696) - 6814
Tephra H1 [2]	612	-	7241 ± 23	-	7949 - 8153	7972 – (8124) - 8360
UCIAMS189841	637	Bulk peat	7925 ± 25	na	8589 - 8951	8547 – (8672) - 8892
UGAMS38373	712	Bulk peat	9360 ± 30	-27.7	10,407 - 10,653	10,272 – (10,499) – 10,701
Beta522335	752	Bulk lacustrine mud	10,520 ± 30	-29.2	12,156 – 12,554	11,921 – (12,301) – 12,569
UCIAMS189840	840	Fine plant material	13,020 ± 50	na	15,289 – 15,743	15,025 – (15,425) – 15,737
UCIAMS189839	882	Fine plant material	13,260 ± 45	na	15,705 - 16,076	15,574 – (16,296) – 17,351

†Calibrated age ranges by Calib 7.1 (Stuiver et al., 1993) and SH13 curve (Hogg et al., 2013).

‡Probability interval of calibrated and median ages from BACON (Blaauw and Christen, 2011).

[1] Mount Burney tephra layer (McCulloch, 1994)

[2] Volcán Hudson tephra layer (Stern et al., 2016)

Table caption

Table 1. Radiocarbon and calibrated age ranges. The weighted mean ages from the BACON Bayesian age model have been used to constrain the Caleta Eugenia record.

Figure captions

Figure 1. Fuego-Patagonia. The principal vegetation zones and isohyets are from Tuhkanen et al., (1989–1990) modified with vegetation mapping by Pisano (1994). Palaeoecological sites mentioned in the text are: ① Cta. Eugenia ② Cta. Robalo; ③ Pto. Harberton; ④ Pta. Moat; ⑤ Valle Andorra, Ushuaia I, II and III; ⑥ Cañadon del Toro and Lapataia; ⑦ Cta. Lacroix, Isla de los Estados; ⑧ Terra Australis; ⑨ La Correntina; ⑩ Lago Yehuin; ⑪ Pta. Yartou; ⑫ Lago Lynch; ⑬ Pto. del Hambre. Archaeological sites mentioned in the text are: (TA) Tres Arroyos; (M) Bahía Mejillones; (T) Tunel; (BC) Imiwaia I and Binushmuka I – Bahía Cambaceres.

Figure 2. The site at Caleta Eugenia. The storm ridges are highlighted by the arcuate strips of shrub vegetation. Inset: oblique image of the mire site at Caleta Eugenia (source: Google Earth 2019).

Figure 3. The Caleta Eugenia profile: sediment stratigraphy, organic content determined by LOI_{550}, and the LPAZs determined from the percentage pollen diagram (Fig. 4) by CONISS alongside the BACON age–depth model.

Figure 4. Caleta Eugenia summary percentage pollen and spore diagram. *Misodendrum* is included in the trees group as it is a hemiparasite of *Nothofagus* trees.

Figure 5. Caleta Eugenia pollen accumulation rate (influx) for selected taxa.

Figure 6. Caleta Eugenia percentage pollen preservation diagram and charcoal accumulation rate (influx).

Figure 1

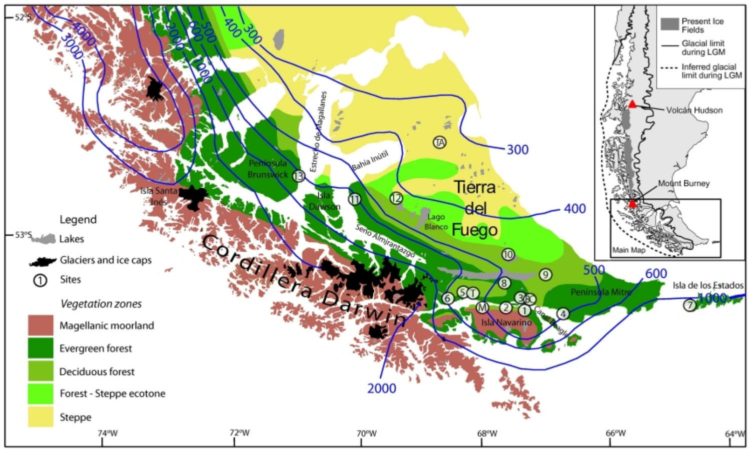

296x209mm (300 x 300 DPI)

Figure 2

296x209mm (300 x 300 DPI)

Figure 3

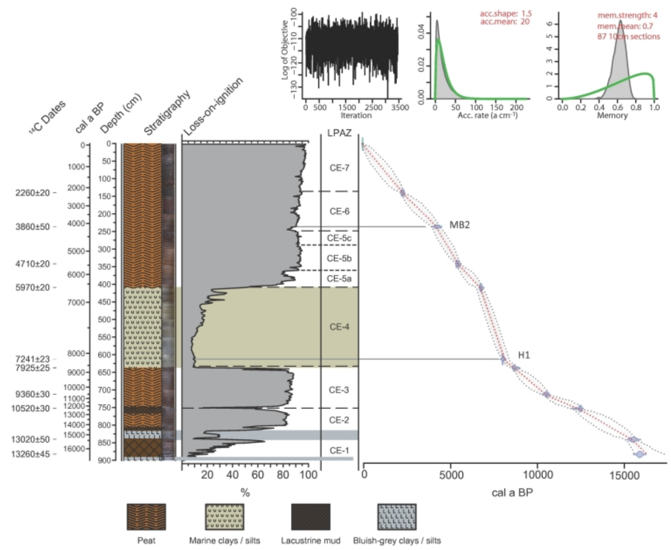

209x296mm (300 x 300 DPI)

Figure 4

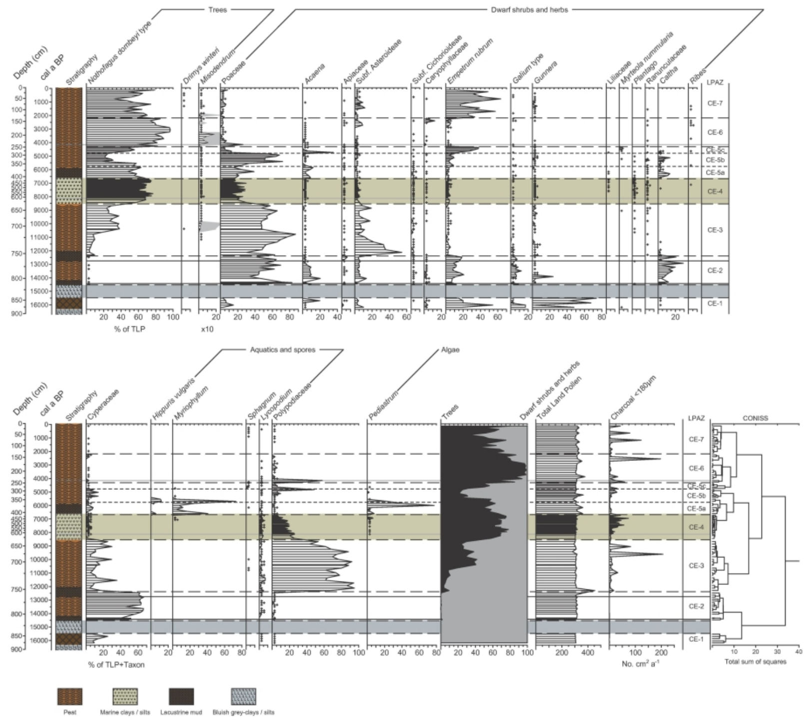

209x296mm (300 x 300 DPI)

Figure 5

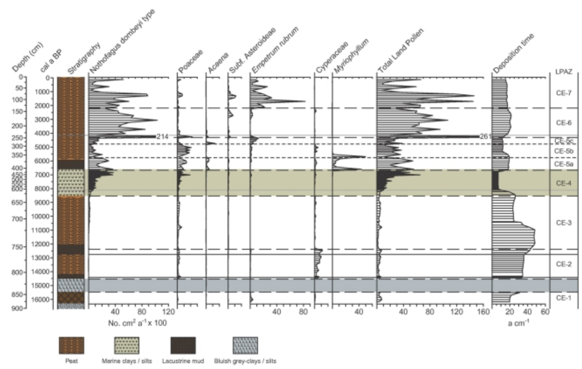

209x296mm (300 x 300 DPI)

Figure 6

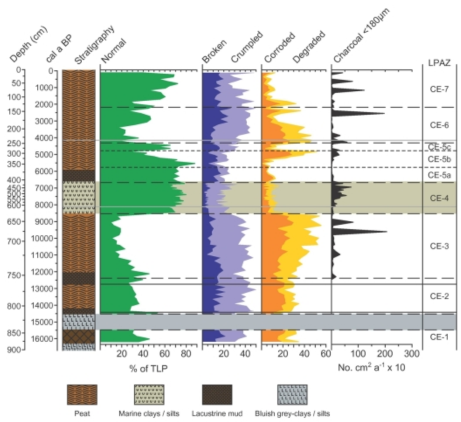

209x296mm (300 x 300 DPI)

Table S1: Tephra geochemistry

	Na_2O	MgO	Al_2O_3	K_2O	CaO	FeO	SiO_2	P_2O_5	TiO_2	MnO	Total
MB2											
1	4.489	0.309	12.284	1.549	1.590	1.373	75.746	0.033	0.230	0.036	97.6
2	4.558	0.332	12.723	1.533	1.729	1.219	77.637	0.037	0.226	0.050	100.0
3	4.496	0.259	12.433	1.652	1.583	1.207	77.518	0.025	0.198	0.038	99.4
4	4.550	0.244	12.017	1.565	1.596	1.209	76.649	0.033	0.208	0.032	98.1
5	4.342	0.331	12.461	1.637	1.759	1.368	77.765	0.039	0.222	0.042	100.0
6	4.588	0.288	12.480	1.636	1.572	1.354	77.351	0.028	0.202	0.046	99.5
7	3.488	0.166	12.022	3.995	1.084	0.825	74.903	0.019	0.128	0.015	96.6
8	4.493	0.333	12.422	1.683	1.740	1.224	76.616	0.037	0.234	0.041	98.8
9	4.398	0.286	12.130	1.475	1.619	1.183	76.660	0.038	0.219	0.039	98.0
10	3.325	0.169	11.898	3.948	0.989	0.872	76.558	0.017	0.131	0.029	97.9
11	4.665	0.293	12.442	1.519	1.650	1.289	76.990	0.032	0.221	0.034	99.1
12	4.442	0.361	13.047	1.630	1.800	1.373	77.649	0.044	0.237	0.024	100.6
H1											
1	5.507	1.644	15.299	2.709	3.260	5.075	63.280	0.364	1.245	0.162	98.5
2	5.944	1.119	15.332	3.026	2.387	3.804	65.215	0.320	1.170	0.140	98.5
3	5.712	1.550	15.521	2.870	3.166	5.031	64.220	0.341	1.235	0.190	99.8
4	5.655	1.633	15.497	2.728	3.116	4.994	62.925	0.431	1.306	0.165	98.4
5	5.595	1.182	15.450	3.073	2.583	4.297	66.814	0.329	1.179	0.153	100.7
6	5.944	1.199	15.711	2.893	2.770	4.228	64.502	0.381	1.261	0.138	99.0
7	5.627	1.323	15.574	3.060	2.911	4.784	65.575	0.309	1.155	0.176	100.5
8	5.504	1.615	15.152	2.981	3.287	5.146	63.079	0.357	1.216	0.172	98.5
9	5.838	1.413	15.200	2.781	2.989	5.088	63.961	0.318	1.182	0.170	98.9
10	5.770	2.420	14.887	2.627	3.782	5.324	63.487	0.393	1.299	0.200	100.2
11	5.854	1.653	15.529	2.743	3.080	4.834	62.637	0.358	1.159	0.148	98.0
12	5.726	1.479	15.532	2.958	2.994	4.800	63.269	0.348	1.205	0.144	98.5
13	5.670	1.326	15.447	3.050	2.779	4.388	63.959	0.293	1.172	0.152	98.2
14	5.976	1.189	15.253	3.139	2.559	4.546	64.479	0.297	1.111	0.170	98.7

Cameca SX100 Electron Microprobe
Column conditions: Cond 1: 15keV 2nA, Cond 2: 15keV 80nA
Condition 1: Na Ka, Mg Ka, Al Ka, K Ka, Ca Ka, Fe Ka, K Ka, Ca Ka, Si Ka
Condition 2: P Ka, P Ka, Ti Ka, Mn Ka, Ti Ka